Nonredundant Functions of αβ and γδ T Cells in Acrolein-Induced Pulmonary Pathology

Michael T. Borchers,*,†,[1] Scott C. Wesselkamper,* Bryan L. Eppert,* Gregory T. Motz,* Maureen A. Sartor,‡ Craig R. Tomlinson,* Mario Medvedovic,‡ and Jay W. Tichelaar*

*Department of Environmental Health, Division of Environmental Genetics and Molecular Toxicology; †Department of Internal Medicine, Division of Pulmonary and Critical Care; and ‡Department of Environmental Health, Division of Biostatistics, University of Cincinnati, College of Medicine, Cincinnati, Ohio 45267

Acrolein exposure represents a significant human health hazard. Repeated acrolein exposure causes the accumulation of monocytes/macrophages and lymphocytes, mucous cell metaplasia, and epithelial injury. Currently, the mechanisms that control these events are unclear, and the relative contribution of T-cell subsets to pulmonary pathologies following repeated exposures to irritants is unknown. To examine whether lymphocyte subpopulations regulate inflammation and epithelial cell pathology, we utilized a mouse model of pulmonary pathology induced by repeated acrolein exposures. The role of lymphocyte subsets was examined by utilizing transgenic mice genetically deficient in either αβ T cells or γδ T cells, and changes in cellular, molecular, and pathologic outcomes associated with repeated inhalation exposure to 2.0 and 0.5 ppm acrolein were measured. To examine the potential functions of lymphocyte subsets, we purified these cells from the lungs of mice repeatedly exposed to 2.0 ppm acrolein, isolated and amplified messenger RNA, and performed microarray analysis. Our data demonstrate that αβ T cells are required for macrophage accumulation, whereas γδ T cells are critical regulators of epithelial cell homeostasis, as identified by epithelial cell injury and apoptosis, following repeated acrolein exposure. This is supported by microarray analyses that indicated the T-cell subsets are unique in their gene expression profiles following acrolein exposures. Microarray analyses identified several genes that may contribute to phenotypes mediated by T-cell subpopulations including those involved in cytokine receptor signaling, chemotaxis, growth factor production, lymphocyte activation, and apoptosis. These data provide strong evidence that T-cell subpopulations in the lung are major determinants of pulmonary pathology and highlight the advantages of dissecting their effector functions in response to toxicant exposures.

Key Words: inflammation; lung injury; macrophage; acrolein; microarray.

[1] To whom correspondence should be addressed at Division of Environmental Genetics and Molecular Toxicology, Department of Environmental Health, University of Cincinnati College of Medicine, Cincinnati, OH 45267-0056. Fax: (513) 558-0925. E-mail: michael.borchers@uc.edu.

Repeated exposure to pulmonary irritants results in several adverse outcomes associated with injury to the airways including inflammation, mucous cell development, and epithelial cell death. The current paradigm is that pulmonary irritants cause damage to the epithelium lining the airways, which generate signals capable of recruiting and activating inflammatory cells (neutrophils, macrophages, and lymphocytes) that exacerbate the epithelial injury. Although many studies have focused on the role of macrophages and neutrophils in these processes, few data exist examining the role of pulmonary lymphocytes in the initiation and perpetuation of pathologies following irritant exposures. T cells play a significant role in acute inflammation and the maintenance of epithelial integrity following acute nonpathogenic insults (Bleavins *et al.*, 1995; Chen *et al.*, 1995; Dziedzic and White, 1987; King *et al.*, 1999). However, the mechanisms whereby T cells are activated and their specific effector functions in response to irritant exposure have received limited attention. The reasons for which are probably both historical and technical. The T cell is traditionally viewed as mediating acquired and innate immunity in response to pathogens. In addition, T cells are neither an abundant cell type in the lung nor are they easily isolated and studied.

Acrolein ($CH_2=CHCHO$) is a highly reactive, low-molecular weight, unsaturated aldehyde known to cause pulmonary inflammation, respiratory tract injury, and suppress pulmonary host defense against infection (Leikauf, 2002). We have demonstrated that persistent acrolein exposure in mice recapitulates several of these pathologies including increased macrophage accumulation, epithelial damage, airspace enlargement, and mucus hypersecretion (Borchers *et al.*, 1999; Borchers *et al.*, 2007a). Acrolein exposures result from exogenous sources (i.e., fuel combustion, wood burning, tobacco smoke) and endogenous formation (generated by oxidative stress in tissues) (see review, Stevens and Maier, 2008). Although the molecular effects of acrolein in the context of acute toxicity have been described (Kehrer and Biswal, 2000), the effects of chronic, *in vivo* acrolein exposure on

T-cell effector functions have not been examined. In this study, we utilized a mouse model of pulmonary pathology induced by repeated acrolein exposures to determine whether pulmonary lymphocyte subpopulations exhibit distinct effector functions in the regulation of inflammation and epithelial cell pathology. The two major aims of the study were to (1) determine the role of αβ and γδ pulmonary lymphocytes in inflammation and epithelial injury following repeated acrolein exposures, and (2) examine the gene expression profiles from purified pulmonary T-cell subpopulations following repeated acrolein exposures. Utilizing animal models deficient in T-cell subsets, cell sorting techniques that allow for the purification of 99% pure cell populations, and microarray technology that allows for the simultaneous analysis of > 30,000 genes, we were able to assess the effects of environmental exposures on T-cell function, and the potential impact of these effects on the pathogenesis and susceptibility to chronic pulmonary diseases. Our results demonstrate a clear distinction between the roles of αβ and γδ T-cell subpopulations in the modulation of pulmonary pathologies following repeated irritant exposures.

METHODS

Animals. Wild-type mice (C57BL/6J) and mice deficient in γδ T cells (B6.129P2-Tcrd[tm1Mom]) and αβ T cells (B6.129P2-Tcrb[tm1Mom]) were purchased from The Jackson Laboratory (Bar Harbor, ME). Tcrd[tm1Mom] and Tcrb[tm1Mom] mice have been backcrossed > 10 generations with C57BL/6J mice. All procedures were conducted using female animals 8–12 weeks of age maintained in ventilated microisolator cages housed in an American Association for Accreditation of Laboratory Animal Care-accredited animal facility. Protocols and studies involving animals were conducted in accordance with the National Institutes of Health.

Acrolein exposure. Animals were exposed to acrolein as previously described (Borchers *et al*., 1998). Acrolein vapor was generated by passing N₂ (3–15 ml/min) over a 3-ml reservoir of liquid acrolein (SigmaAldrich, St Louis, MO). This mixture was diluted with high-efficiency particle-filtered air (400 ml/min) and introduced into a 0.32-m³ stainless steel chamber. The exposure concentration was analyzed using a method described by Cohen (1961). The chamber atmosphere was sampled with a series of two glass-fritted impingers, each containing 10 ml of 96% ethanol. A fraction of each sample was mixed with 50mM hexylresorcinol (Sigma, St Louis, MO), 2.1mM mercury chloride (Aldrich, Milwaukee, WI), and 29.7M trichloroacetic acid (Fisher, Fair Lawn, NJ). Samples and known standards in equal volumes were heated (65°C for 15 min) and allowed to cool (22°C for 15 min), and the absorbance at 605 nm was measured with a spectrophotometer (Beckman DU-64). Exposures were measured twice each day. Daily fluctuations over the 6-h exposures did not exceed 10%, and the average exposure concentrations were within 5% of the target concentration.

Mucous cell metaplasia. Mucous cell development along the airway epithelium was quantified in paraffin-embedded tissue sections (5 μm) stained with periodic acid-Schiff reagent. Parasaggital sections were analyzed by bright-field microscopy with an image analysis software program (ImagePro Plus, Media Cybernetics, Silver Spring, MD) to derive an airway mucus index that is reflective of both the amount of mucus per airway and the number of airways affected. The airway mucus index was calculated by summing the ratio of the periodic acid-Schiff-positive epithelial area to the total epithelial area per section and then dividing by the number of airways per section (Borchers *et al*., 2001).

BAL mucin assay. MUC5AC mucin in the airways was determined using an enzyme-linked immunosorbent assay (ELISA) modified from Miller *et al*. (2002). Briefly, 100 μl of bronchoalveolar lavage (BAL) sample was dried overnight at 37°C onto 96-well microtiter plates (Immulon, PGC Scientific, San Diego, CA), washed and incubated with a biotinylated primary anti-MUC5AC antibody (LabVision, Fremont, CA) followed by an incubation with a secondary peroxidase-conjugated antibody. A standard curve was generated using BAL fluid from rats exposed to 2.0 ppm acrolein, 6 h/day, for 10 days.

Bronchoalveolar lavage. After exposure, mice were anesthetized (50 mg/kg of Nembutal i.p. [Henry Schein, Indianapolis, IN]) and exsanguinated by severing the posterior abdominal aorta. The lungs were then lavaged two times with 1 ml of Hanks' balanced salt solution (HBSS). Individual BAL returns were pooled and centrifuged at 1000 × g, 10 min. The supernatant was removed and stored at −70°C until assayed for mucin activity. The cell pellet was reconstituted in 1 ml of HBSS containing 2% fetal bovine serum (FBS).

Cell enumeration and differential counts. Total cell counts were determined with a hemocytometer. Differential cell counts (> 300 cells) were performed on PROTOCOL Hema3-stained (Fisher Diagnostics, Middletown, VA) cytospin slides (Cytospin3, Shandon Scientific, Waltham, MA) from 250 μl of lavage fluid. Data are presented as total cells after adjusting for volume recovered.

Tissue fixation, histology, immunohistochemistry. After exposure, animals were euthanized as described previously. To obtain tissue for histological analysis, a cannula was inserted in the middle of the trachea, and the lung was instilled with 10% phosphate-buffered formalin (20 cmH₂O for 1 min). The trachea was ligated, and the inflated lung was immersed in fixative for 24 h. The fixed tissues were dissected after 24 h, and washed with phosphate-buffered saline (PBS), dehydrated through graded ethanol solutions (30–70%), and processed into paraffin blocks (Hypercenter XP, Shandon). Activate CASPASE 3 (CASP3) protein was detected with a rabbit polyclonal antibody (R&D Systems, Minneapolis, MN) in paraffin sections (5 μm) of mouse airways as previously described (Borchers *et al*., 2007b). Antigen-antibody complexes were detected with the Vectastain ABC Peroxidase Elite goat IgG kit (Vector Laboratories, Burlingame, CA). Endogenous peroxidase was quenched (15 min at 22°C) with 3% H₂O₂ in methanol. The sections were incubated in 2% normal goat serum in PBS with 0.2% Triton X-100 (blocking solution; 2 h at 22°C) and incubated (20 h at 4°C) with primary antibody (1:15,000 dilution). The sections were washed (6 × 5 min) in PBS with 0.2% Triton X-100 and incubated (30 min at 22°C) with biotinylated goat anti-chicken antibody (1:2000 dilution). The sections were treated (15 min at 22°C) with the avidin-biotin blocking kit (Vector Laboratories) to block endogenous biotin in the tissue. The sections were incubated with the avidin-biotin-peroxidase complex diluted in blocking solution (30 min at 22°C), nickel diaminobenzidine in 0.1M acetate buffer (4 min at 22°C) for development of a colored reaction product, and Tris-cobalt (4 min at 22°C) and counterstained with 0.1% nuclear fast red (2 min at 22°C).

T-cell purification. Lungs were perfused through the right ventricle and the tissue was enzymatically digested as previously reported (Borchers *et al*., 2001). Single cell suspensions from perfused, digested lungs were layered onto a single-step Percoll gradient (60% Percoll [ρ = 1.084], 1× HBSS, 15mM N-(2-hydroxyethyl)-piperazine-N′-2-ethanesulfonic acid [pH 7.4]) and centrifuged (45 min, 2000 × g, 4°C). The buffy coat containing mononuclear cells was removed and washed twice in PBS containing 2% FBS. The cell pellet was then subject to red blood cell lysis, washed, and resuspended in PBS containing 2% FBS. Cell sorting using a BD FACSVanatge flow cytometer subsequently isolated T cells. To isolate T-cell subsets, cells were labeled with antibodies against CD3 (clone 145-2C11, PharMingen, San Diego, CA), T-cell receptor (TCR) β (clone H57-597, PharMingen) and TCR δ (clone GL3, PharMingen). Cells dual positive for CD3 and TCR β were isolated into a separate tube from the cells that were dual positive for CD3 and TCR δ. The purity of the isolated cells was determined by flow cytometry performed on a FACScan cytofluorometer (Becton Dickinson, Franklin Lakes, NJ). Data acquisition and analysis were performed using CellQuest software (Becton Dickinson).

RNA isolation and amplification. Total cellular RNA from purified lymphocyte populations was isolated with a column-based procedure using the RNEasy Micro kit (Qiagen, Valencia, CA) in order to obtain a maximum yield from a very small amount starting material. To obtain enough RNA for microarray analysis, two rounds of linear amplification of the total RNA using the Amino Allyl MessageAmp II aRNA Amplification kit (Ambion, Austin, TX) were performed. In summary, first strand cDNA is synthesized using a reverse transcriptase enzyme and the T7 oligo dT primer in order generate cDNA with the T7 promoter sequence attached. DNA polymerase and RNASe H are added to synthesize second strand cDNA and degrade RNA. A cDNA purification procedure utilizing a column-based technique removed RNA, salts, primers, and enzymes. The templates were amplified in the first round by *in vitro* transcription using the T7 polymerase and unlabeled primers. Following another round of purification, the *in vitro* transcription was performed identically to the first round except amino allyl UTP was substituted for the unlabeled UTP, thus allowing for subsequent Cy3 and Cy5 conjugation. The amplified RNA was again purified on a column and tagged with the appropriate fluorescent dye as detailed below.

Microarray experimental design. T-cell subpopulations were purified from lung tissue on six separate occasions ($n = 4$ sham-exposed and 4 acrolein-exposed $\gamma\delta$ T-cell samples; $n = 6$ sham-exposed and 6 acrolein-exposed $\alpha\beta$ samples). Lymphocytes from four mice were pooled for each isolation and represented a single RNA sample. Ten arrays (four $\gamma\delta$ T cell, six $\alpha\beta$ T cell) were performed and analyzed as subsequently described. Each array contained 10 μg of amplified RNA from a sham-exposed and an acrolein-exposed RNA sample.

The analysis of the microarray data consisted of the following components: (1) the evaluation of global expression changes in $\alpha\beta$ T cells from the lungs of sham-exposed mice compared with $\alpha\beta$ T cells from the lungs of 1-week acrolein-exposed (2.0 ppm) mice, (2) the evaluation of global expression changes in $\gamma\delta$ T cells from the lungs of sham-exposed mice compared with $\gamma\delta$ T cells from the lungs of 1-week acrolein-exposed (2.0 ppm) mice, (3) validation of changes in 15 candidate genes by quantitative real-time PCR, and (4) comparison of significant transcript changes between $\alpha\beta$ and $\gamma\delta$ T cells following acrolein exposures. We chose a 1-week exposure period for these studies because this was the earliest time point at which two important phenotypes (i.e., epithelial cell injury, and macrophage inflammation) were significantly changed in the C57BL/6J mice and corresponding alterations were first evident in the T-cell knockout mice.

Microarray hybridization. Microarray analysis was conducted in the Genomics and Microarray Core Facility at the University of Cincinnati, which is housed in our Department of Environmental Health. The following references provide a detailed protocol for the procedure (Wesselkamper *et al.*, 2005). Briefly, RNA quality was assessed and quantified by analysis with an Agilent Bioanalyzer (Quantum Analytics, Inc., Foster City, CA). To examine differential gene expression of 31,775 70-mer oligonucleotides, a microarray was fabricated by the Genomic and Microarray Laboratory, Center for Environmental Genetics, University of Cincinnati (http://microarray.uc.edu/), using a commercial library (Qiagen-Operon, Alameda, CA). Clones (70 mers) from the Operon Library were amplified by polymerase chain reaction (PCR), printed onto glass slides (Omnigrid Microarrayer; GeneMachines, San Carlos, CA). Each sample was randomly reciprocally tagged with fluorescent cyanine 3 (Cy3) or cyanine 5 (Cy5; e.g., Cy3 for control and Cy5 for exposed). Cy3 and Cy5 samples were cohybridized with the printed 70 mers. After hybridization, slides were washed and scanned at 635 (Cy5) and 532 (Cy3) nm (GenePix 4000B; Axon Instruments, Inc., Union City, CA). Imaging and data generation were carried out using a GenePix 4000A and GenePix 4000B and associated software from Axon Instruments, Inc. (Foster City, CA). The microarray slides were scanned with dual lasers with wavelength frequencies to excite Cy3 and Cy5 fluorescence emittance. Images were captured in JPEG and TIFF files, and DNA spots captured by the adaptive circle segmentation method.

Microarray analysis. The data representing background subtracted spot intensities generated by GenePix Pro version 5.0 software was analyzed to identify differentially expressed genes. Data normalization was performed in two steps for each microarray separately. First, background adjusted intensities were log-transformed and the differences (R) and averages (A) of log-transformed values were calculated as $R = \log_2(X1) - \log_2(X2)$ and $A = [\log_2(X1) + \log_2(X2)]/2$, where X1 and X2 denote the Cy5 and Cy3 intensities after subtracting local backgrounds, respectively. Second, normalization was performed by fitting the array-specific local regression model of R as a function of A. Normalized log-intensities for the two channels were then calculated by adding half of the normalized ratio to A for the Cy5 channel and subtracting half of the normalized ratio from A for the Cy3 channel. Statistical analyses were performed for each T-cell population independently by fitting the following mixed effects linear model for each gene: $Y_{ijk} = \mu + A_i + S_j + C_k + \varepsilon_{jk}$, where Y_{ijk} corresponds to the normalized log intensity on the ith array, labeled with the kth dye ($k = 1$ for Cy5 and $k = 2$ for Cy3) and for the jth treatment. μ is the overall mean log intensity, A_i is the effect of the ith array, S_j is the effect of the jth treatment, C_k is the effect of the kth dye, and ε_{ijk} is the random experimental error associated with Y_{ijk}. Array effects were treated as random effects, whereas treatment and dye effects were treated as fixed (Wolfinger *et al.*, 2001). Resulting t-statistics for estimating exposed versus control differences ($j = 2$ vs. $j = 1$) were modified using an empirical Bayesian moderated-T method (Smyth, 2004). Estimates of fold-change were calculated, and genes with p value < 0.005, with a fold-change > 2.0, and having an average intensity > 50 were considered significantly differentially expressed (659 transcripts in $\alpha\beta$, 626 transcripts in $\gamma\delta$). For exposed versus control comparisons, this $p < 0.005$ cutoff corresponded to an estimated false discovery rate < 0.09 in $\gamma\delta$ and ≤ 0.10 in $\alpha\beta$ T-cell subsets. From the 1093 transcripts identified as differentially expressed in at least one of the two T-cell subpopulations, a transcript was defined as changed in both groups if *both* p values < 0.005. Data normalization and statistical analyses were performed using SAS statistical software package (SAS Institute Inc., Cary, NC).

Quantitative real-time PCR. To obtain RNA for validation of genes identified by microarray analysis, additional T-cell subpopulations were purified from lung tissue on separate occasions as described above ($n = 3$ sham-exposed and 3 acrolein-exposed $\gamma\delta$ T-cell samples; $n = 3$ sham-exposed and 3 acrolein-exposed $\alpha\beta$ samples). Lymphocytes from four mice were pooled for each isolation and represent a single RNA sample. Total RNA was isolated from lung lymphocytes, and quantitative real-time PCR (qRT-PCR) was performed on an ABI 7600 System using prevalidated TaqMan Gene Expression Assays according to manufacturer's protocols (Applied Biosystems). Data are expressed as fold increase over control calculated by the $2^{-\Delta\Delta CT}$ method (RQ Software, Version 1.4, Applied Biosystems, Foster City, CA).

Statistics. Normally distributed data (excluding the microarrays) were analyzed for statistical significance by using one-way ANOVA with differences between means considered significant when $p < 0.05$.

RESULTS

Acrolein-Induced Pulmonary Pathologies

Repeated acrolein exposures caused the development of mucous cell metaplasia in a time-dependent manner. Significant increases in the number of Periodic acid-Schiff's (PAS)–positive epithelial cells were evident in all strains examined following two weeks of exposure and these increases were persistent following four weeks of exposure. Mucous cell development was restricted to the largest airways of mice and there were no differences observed between the $\alpha\beta$- and $\gamma\delta$-deficient strains (Fig. 1). These histological findings are consistent with the results obtained from analysis of mucin glycoprotein in the BAL fluid. To determine whether
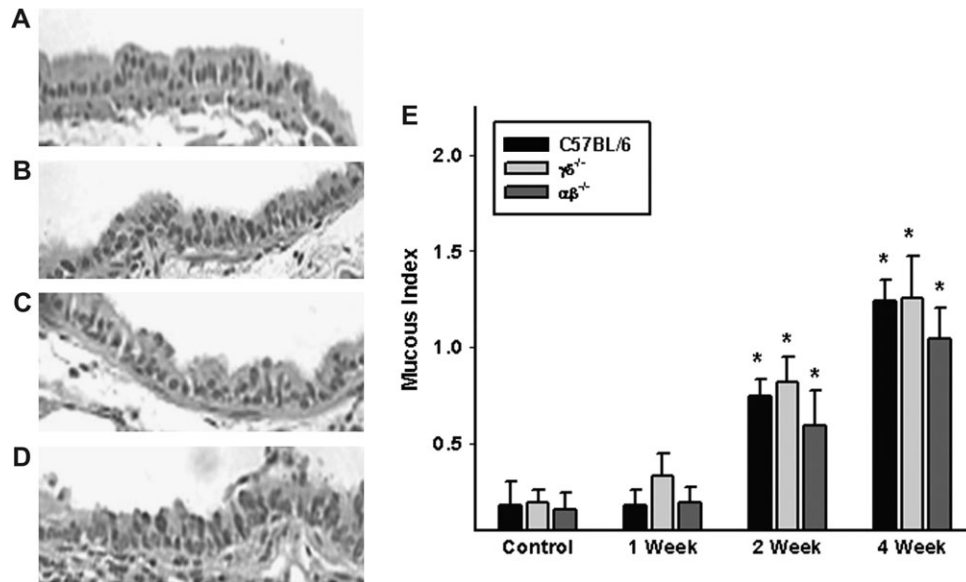
FIG. 1. Mucous cell metaplasia develops in mice following repeated acrolein exposure. Mucous cell metaplasia along the airways was visualized by light microscopy of PAS stained lung sections. (A) C57BL/6J control, (B) C57BL/6J 4 weeks, (C) $\gamma\delta^{-/-}$ 4 weeks, (D) $\alpha\beta^{-/-}$ 4 weeks. Images are representative of $n = 8$ mice per group. (E) Quantitation of mucus cell metaplasia following repeated acrolein exposure. Values are means ± SE of evaluations performed in duplicate as independent observer-blinded assessments; $n = 8$ mice/group. *Significantly different from strain-matched control, $p < 0.05$.

significant hypersecretion occurs in response to acrolein, we developed an ELISA-based method to assay MUC5AC mucin glycoprotein in the BAL of mice. ELISA data demonstrate that none of the samples from mouse BAL were positive for MUC5AC mucin glycoprotein at any time points (data not shown).

BAL Epithelial Cells

Acrolein exposures caused a significant increase in epithelial cell sloughing in the C57BL/6J mice and $\gamma\delta$-deficient mice, but not $\alpha\beta$-deficient mice (Fig. 2). An approximate twofold increase in the number of ciliated epithelial cells recovered in the BAL of C57BL/6J mice was evident after repeated exposure to 2.0 ppm acrolein. This effect was observed at 1 week and persisted for up to 4 weeks of exposures. $\gamma\delta$-deficient mice had a significantly higher level of epithelial cells in the BAL at all times examined compared with the C57BL/6J mice. $\gamma\delta$-deficient mice repeatedly exposed to 2.0 ppm acrolein demonstrated an eightfold increase in the number of ciliated epithelial cells recovered in the BAL after 1 week of exposures. The response in $\gamma\delta$-deficient mice was greatest following 1 week of exposures with a slight decline at both 2 and 4 weeks of exposure (but still significantly greater than C57BL/6J mice). In contrast, $\alpha\beta$-deficient mice did not exhibit a significant increase in epithelial cell sloughing following any of the exposure periods. In response to 0.5 ppm, significant sloughing of epithelial cells in the BAL was only observed in the $\gamma\delta$-deficient mice and was significantly greater than that of sham-exposed $\gamma\delta$-deficient mice and 0.5 ppm acrolein-exposed C57BL/6J mice at all times examined.

Apoptosis of Pulmonary Epithelial Cells

Immunohistochemistry was performed on tissue sections to complement the BAL assessment of the magnitude of epithelial cell damage in the airways. We utilized an antibody against active CASPASE 3 (CASP3), a marker of apoptosis, to determine the extent and localization of cellular injury. These results demonstrate that apoptosis occurs in the terminal bronchioles and alveolar epithelium in response to 2.0 ppm acrolein exposure. Consistent with the BAL epithelial cell data, acrolein exposures cause a significant increase in apoptosis in the C57BL/6J mice and $\gamma\delta$-deficient mice, but not $\alpha\beta$-deficient mice (Fig. 3). Furthermore, $\gamma\delta$-deficient mice had a significantly higher level of CASP3 positive cells and were significantly increased more rapidly compared with the C57BL/6J mice.

Pulmonary Inflammation

Exposures to 2.0 ppm acrolein resulted in a persistent increase in macrophage accumulation in the lungs of C57BL/6J mice (Fig. 4). $\gamma\delta$-deficient mice exhibited an increase in macrophage accumulation following 2 and 4 weeks of 2.0 ppm acrolein exposures which was significantly lower than C57BL/6J mice. In contrast, $\alpha\beta$-deficient mice failed to exhibit an increase in macrophage accumulation following any of the exposure periods. In response to 0.5 ppm acrolein, C57BL/6J mice exhibited a significant increase in macrophage accumulation after 2 and 4 weeks of exposure (Fig. 4). This increase in macrophage accumulation in response to 0.5 ppm acrolein was only 50–60% greater than sham-exposed controls as compared with 200–250% increase in response to 2.0 ppm acrolein at the
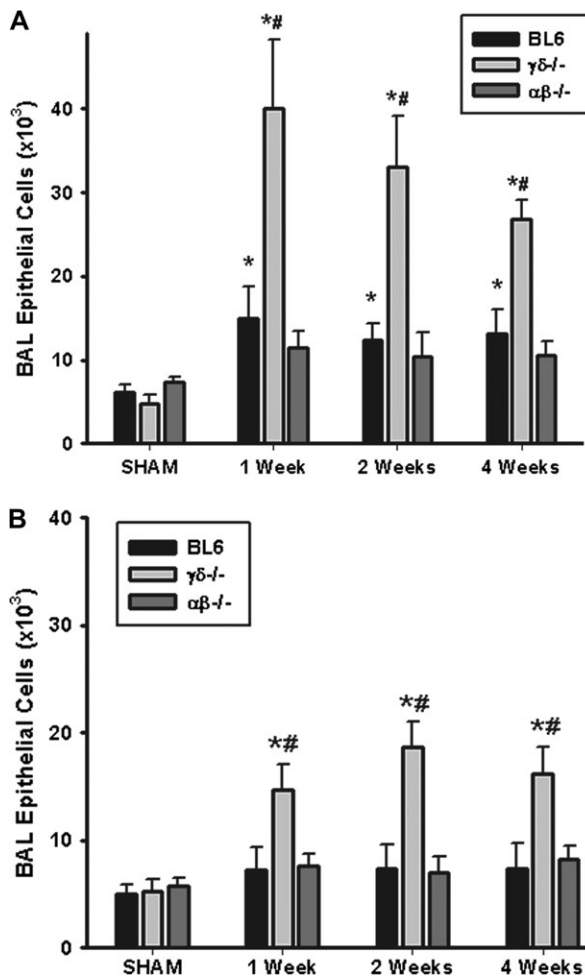
FIG. 2. Airway epithelial cell injury in mice following acrolein exposure. The accumulation of epithelial cells was assessed by enumeration of bronchoalveolar lavage cells in mice exposed to (A) 2.0 or (B) 0.5 ppm acrolein for up to 4 weeks. The number of epithelial cells is a product of the total number of cells recovered and the percentage of epithelial cells as determined by cytocentrifuge preparations (counting $\geq$ 300 cells per slide). Values presented are means ($\pm$ SE) of eight mice per group. *Denotes value significantly greater than strain-matched control at $p < 0.05$. #Denotes value significantly different than exposure-matched C57BL/6J mice at $p < 0.05$.

same time points. Nearly identical results were observed in γδ-deficient mice. No significant changes in macrophage accumulation were observed in αβ-deficient mice at any time points examined.

Neutrophils were the only other cell type consistently found in the BAL of acrolein-exposed mice. However, the numbers of neutrophils were negligible (less than 2%) compared with the numbers of macrophages at all times and doses in all three strains tested. Significant numbers of lymphocytes (< 0.5%) were not detected in the BAL.

Pulmonary Lymphocyte Purification

To begin to examine the contributions of the individual lymphocyte subsets to the observed phenotypes of epithelial cell injury and increased macrophage accumulation, we purified αβ and γδT cells from isolated, perfused, enzymatically digested lung tissue. Purification of the individual cell types was performed using a cell sorting strategy that takes advantage of the fact that αβ and γδ receptor expression is mutually exclusive on T-cell subsets. Using fluorescent-labeled antibodies against the TCR protein CD3, the TCR β subunit, and the TCR δ subunit, we achieved purities of approximately 99% (Fig. 5). This is critical in the analysis of the global transcript repertoires because significant contamination would greatly reduce the power of the microarray studies.

Gene Changes

Analysis of the microarray data revealed 659 genes in αβ T cells isolated from the lungs exhibited significant changes in expression levels following acrolein exposure. Comparably, 626 genes in γδ T cells isolated from the lungs exhibited significant changes in expression levels following acrolein exposure. We identified many genes among these groups that may contribute to the phenotypes observed in acrolein-exposed αβ and γδ T-cell–deficient mice. These candidate genes are listed in Tables 1 and 2. Among these changes we observed genes involved in a diverse group of cellular functions including, but not limited to, cytokine receptor signaling, chemotaxis, growth factor production, lymphocyte activation, and apoptosis.

Specifically, several transcripts involved in macrophage-T cell interactions were upregulated in αβ T cells. These genes included the Interferon γ receptor (*Ifngr*), Interleukin (IL)-18 receptor (*Il18r*), IL-12 receptor (*Il12r*), and IL-3 (*Il3*). All of the ligand:receptor interactions mediated by these genes exhibit defined effector functions involved in macrophage accumulation and activation. Specific transcript changes in γδ T cells that were related to the phenotype of compromised epithelial cell integrity included genes involved in the surveillance of major histocompatibility complex (MHC)-1 receptor expression including killer cell lectin-like receptors (*Klra2*, *Klra9*), toll-like receptor (TLR) signaling (*Hmgb1*, *Daf2*, *Cd14*), genes involved in cytotoxic lymphocyte effector functions (*Mpeg1*, *Cd28*), and genes involved in the resolution of tissue injury and remodeling (*Cd44*, S*erpine1*).

Validation

To verify changes observed in the microarray experiments, we selected 15 genes whose expression was either increased (*Cd97*, *Hmgb1*, *Cxcl2*, *Ifngr2*, *Egr1*, *Ptprc*, *Cd164*, *Chi3l3*, *Il18r1*, *S100a10*) or decreased (*Tnfsf11*, *Egr1*, *Cd164*, *S100a4*, *S100a10*, *Klrc1*) in one or both of the T-cell subsets, or not significantly altered but expressed at high levels (*Irf1*, *Ccl5*). The results of this study indicate that there is generally good agreement between the two methods. Of the 15 genes assayed by quantitative real-time PCR measurements in each cell type, 25 of 30 measurements were supportive of the microarray results (Table 3).
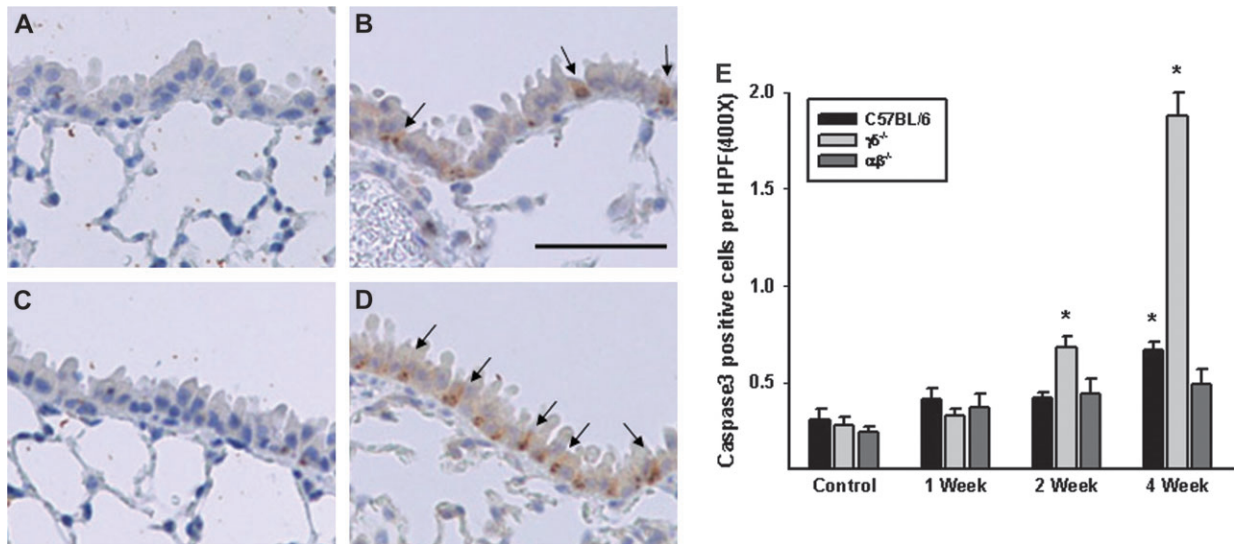
FIG. 3. Increased active CASP3 is greater in the lungs of $\gamma\delta^{-/-}$ mice exposed to acrolein. The accumulation of apoptotic cells in airway epithelial cells of mice was assessed by immunohistochemistry on paraffin-embedded sections using a rabbit antibody specific for active CASP3. (A) Filtered air-exposed C57BL/6J mice, (B) 4-week acrolein-exposed (2.0 ppm) C57BL/6J mice, (C) Filtered air-exposed $\gamma\delta$-deficient mice, and (D) 4-week acrolein-exposed $\gamma\delta$-deficient mice. Photomicrographs (400× original magnification) are representative of $n = 8$ mice per group. (E) Quantitation of active CASP3 in the lungs following 2.0 ppm acrolein exposure. Active CASP3 positive-stained cells were quantified from photomicrographs of lung sections of control and acrolein-exposed mice. Values presented are means ± SE of the number of positive cells per high-powered field (×400). *Denotes value significantly greater than strain-matched controls at $p < 0.05$.

Comparison of Gene Changes

Surprisingly, of the 1285 significant changes in gene expression observed in the two T-cell subsets, only 6% of the changes were consistent between the two subsets. For example, only 2% of significant changes were genes that increased in both $\alpha\beta$ and $\gamma\delta$ T cells, and only 4% of significant changes were genes that decreased in both $\alpha\beta$ and $\gamma\delta$ T cells (Fig. 6). Fifteen percent of the significant changes were genes that increased in $\gamma\delta$ T cells but decreased in $\alpha\beta$ T cells, and 9% of the significant changes were genes that increased $\alpha\beta$ T cells but decreased in $\gamma\delta$ T cells. The remaining 72% of significant changes were unique to only one of the T-cell subsets.

DISCUSSION

This study examined the roles and potential effector functions of the two T-cell populations, $\alpha\beta$ and $\gamma\delta$, that reside in pulmonary tissues following repeated exposure to a ubiquitous air toxicant, acrolein. Using mice genetically deficient in each of these cell types, we have (1) established a role for $\alpha\beta$ T cells in acrolein-induced persistent macrophage accumulation, and (2) established a role for $\gamma\delta$ T cells in the protection of the pulmonary epithelium against necrotic and apoptotic cell death observed in mice following acrolein exposure. Furthermore, we have established a comprehensive database of gene expression in each of the pulmonary lymphocyte subsets, and report T-cell–specific changes in gene expression that will lead to more intensive studies of the mechanisms involved in protection of the lung mucosa following repeated irritant exposure. The data reported here are the first to dissect the roles and responses of individual lymphocyte populations following exposure to air toxics as opposed to pathogens.
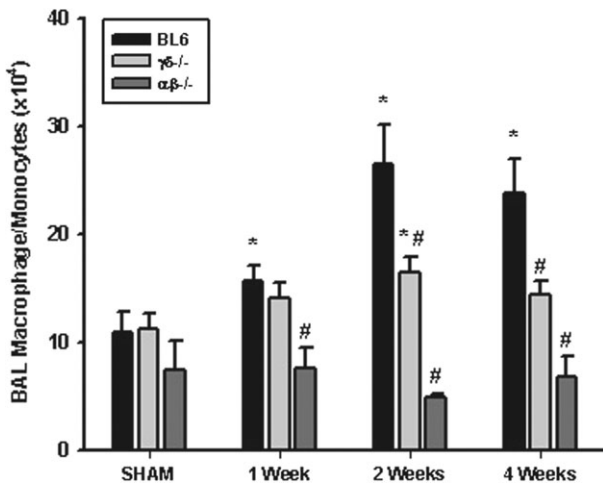
FIG. 4. Macrophage accumulation in the lungs of mice exposed to acrolein. The accumulation of alveolar macrophage was assessed by enumeration of bronchoalveolar lavage cells in mice exposed to (A) 2.0 or (B) 0.5 ppm acrolein for up to 4 weeks. The number of macrophages is a product of the total number of cells recovered and the percentage of macrophages as determined by cytocentrifuge preparations (counting $\geq$ 300 cells per slide). Values presented are means (± SE) of eight mice per group. *Denotes value significantly greater than strain-matched controls at $p < 0.05$. #Denotes value significantly different than exposure-matched C57BL/6J mice at $p < 0.05$.
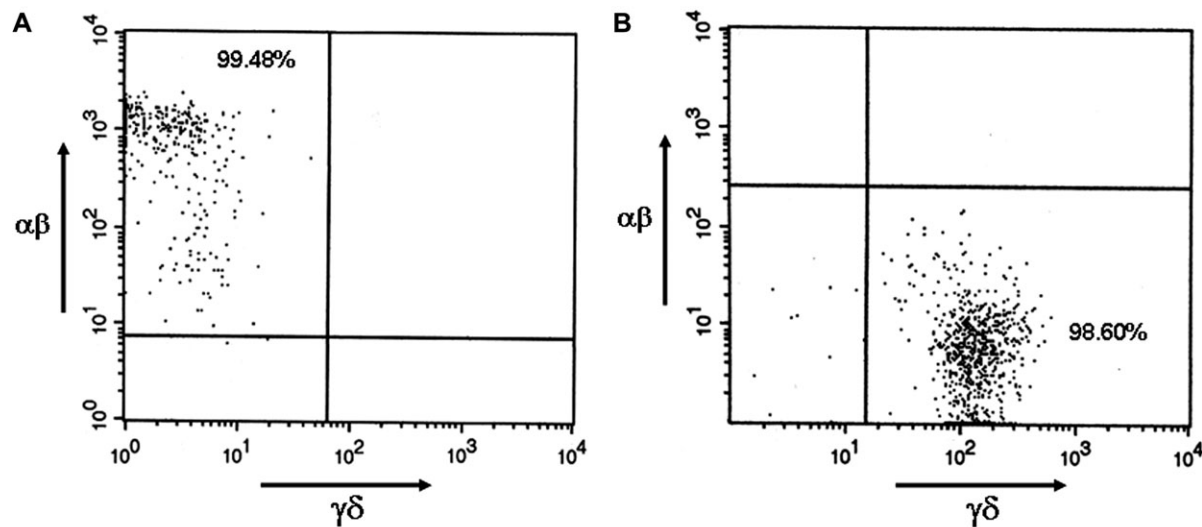
FIG. 5. Isolation and purity of pulmonary αβ and γδ T cells. Cells were isolated from filtered air-exposed and acrolein-exposed (2.0 ppm, 1 week) C57BL/6J mice by enzymatic digestion of perfused lung tissue as detailed in the Methods. The purity of the isolated cells was determined by flow cytometry and is depicted by dot plots that indicate the number of cells that stain positive for either the (A) αβ TCR or the (B) γδ TCR.

Acrolein exposures in the ambient air of the urban environment represent a significant human health hazard. The U.S. Environmental Protection Agency (U.S. EPA) estimates that ambient concentrations of acrolein exceeded the reference concentration in > 90% of the United States in 1999 and exceeded 10 times the reference concentration in > 105 of the United States (U.S. EPA, 2006). Acrolein is proposed to be the noncancer hazardous air pollutant of greatest concern based on health effects and concentrations in the environment (Caldwell *et al.*, 1998). Most recently, Woodruff *et al.* (2007) estimated that ambient concentrations of acrolein represent a significant health risk associated with decreased respiratory function in the United States. Numerous studies have reported the effects of acrolein exposures on several species including mice. In experimental animals, acrolein exposures induce lesions associated with chronic obstructive pulmonary disease. We, and others, have demonstrated that doses of acrolein found in tobacco smoke (Carmines and Rajendran, 2008) are sufficient to induce hallmark features of chronic obstructive pulmonary disease including increased macrophage accumulation, epithelial damage, airspace enlargement, and mucus hypersecretion (Borchers *et al.*, 1999, 2007a; Costa *et al.*, 1986; Feron *et al.*, 1978; Lyon *et al.*, 1970).

The present study expands the previous findings of acrolein-induced epithelial cell hypertrophy and mucous cell development by examining two endpoints of epithelial cell injury: epithelial cell numbers in the BAL, and CASP3 immunoreactivity (apoptosis marker) in formalin-fixed, paraffin-embedded sections of mouse lung. The data derived from the BAL is likely indicative of necrotic cell death in the proximal airways because the majority of the cells (> 90%) are ciliated and fail to exclude trypan blue. Direct injury and subsequent death at

this level of the respiratory tract is likely because the dose of acrolein is greatest in the upper airways and decreases toward the distal respiratory epithelium. The mechanism of cell death in the distal airways is more likely mediated by apoptotic processes cause by either direct injury to the epithelium of indirect mechanisms encompassing efficient removal of injured cells by the immune system. This is supported by the fact that the majority of CASP3 positive cells in the lung following acrolein exposures are localized to the terminal bronchioles.

T cells expressing the γδ TCR are intriguing cells linked to the homeostasis of the lung microenvironment because they localize to the epithelium (Augustin and Sim, 1990) and secrete proinflammatory and chemotactic cytokines, as well as factors that promote epithelial cell growth and repair (Hayday *et al.*, 2001). These T-cell subpopulations are unique in their ability to recognize nonpeptide MHC-1–like antigens expressed on transformed, stressed, or injured epithelial cells (Hayday *et al.*, 2001). They also possess the ability to modulate epithelial cell growth (Boismenu and Havran, 1994), and express epithelial growth factors and an array of cytokines and chemokines that recruit/activate inflammatory cells (Fahrer *et al.*, 2001; Shires *et al.*, 2001). The effect of acrolein exposure on epithelial cell injury in mice devoid of γδ T cells suggests that this cell type is critical in the protection of epithelial cell integrity following irritant exposure. Mice genetically deficient in γδ T cells exhibited a significant increase in the number of sloughed epithelial cells in the airways compared with wild-type mice or mice genetically deficient in αβ T cells. This response was most prevalent at 2.0 ppm acrolein and still evident at 0.5 ppm acrolein (a dose which did not cause significant epithelial cell death in C57BL/6J mice). This conclusion is bolstered by the results obtained from the CASP3 immunohistochemistry.

TABLE 1
Candidate Gene Expression Changes in αβ T Cells following Acrolein Exposures

Accession ID	Gene symbol	Gene name	Description	Avg intensity[a]	Fold induction[b]	p Value
NM_008338	Ifngr2	Interferon gamma receptor 2	Interferon gamma receptor 2	1783	2.76	0.0005
NM_016780	Itgb3	Integrin beta 3	Integrin beta 3, adhesion molecule	4424	2.07	0.003
NM_011311	S100a4	S100 calcium binding protein A4	Antimicrobial	3336	3.00	0.0008
NM_008871	Serpine1	Serine (or cysteine) peptidase inhibitor, clade E, member 1	Serine proteinase inhibitor	329	5.87	0.0007
NM_013520	Flt3l	FMS-like tyrosine kinase 3 ligand	Anti-apoptotic, T-cell proliferation	136	2.42	0.001
NM_013541	Gstp1	Glutathione S-transferase, pi 1	Detoxifying enzyme	4249	2.38	0.0005
NM_008365	Il18r1	Interleukin 18 receptor 1	Interleukin 18 receptor	1613	2.53	0.0009
NM_010556	Il3	Interleukin 3	Macrophage growth/survival factor	393	2.72	0.001
NM_008353	Il12rb1	Interleukin 12 receptor, beta 1	Interleukin 12 receptor	112	2.46	0.001
NM_011925	Cd97	CD97 antigen	Adhesion/activation of leukocytes	1246	2.23	0.002
NM_174851	Il28ra	Interleukin 28 receptor alpha	Interleukin 28 receptor	385	2.36	0.001
NM_021099	Kit	kit oncogene	Thymocyte differentiation	51	2.19	0.001
NM_007522	Bad	Bcl-associated death promoter	Apoptosis antagonist	758	2.22	0.003
NM_010336	Edg2	Endothelial differentiation, lysophosphatidic acid G-protein–coupled receptor, 2	Lysophosphatidic acid receptor	123	−3.56	0.002
NM_013493	Cnbp1	Cellular nucleic acid binding protein	Cellular nucleic acid binding protein	6660	−3.02	0.0002
NM_007610	Casp2	Caspase2	Proapoptotic enzyme	843	−2.50	0.002
AF106008	Klrc1	Killer cell lectin-like receptor subfamily C, member 1	Killer cell lectin-like receptor	164	−2.66	0.003
NM_019777	Ikbke	Inhibitor of nuclear factor kappa-B kinase epsilon subunit	Inhibitor of NF-κB kinase	226	−2.32	0.003

[a]Average intensity is an arbitrary value derived from the fluorescence intensity of the microarray analysis.
[b]Fold induction is the ratio of acrolein-exposed to sham-exposed values.

CASP3-positive cells initially increased (~2-fold) in the γδ-deficient mice following 2 weeks of acrolein exposure and increased further at 4 weeks (~8-fold). In contrast, C57BL/6J mice exhibited a significant increase only following 4 weeks exposure to 2.0 ppm, and αβ-deficient mice, although exhibiting a trend of increasing CASP3, did not demonstrate statistically significant staining at any time points.

The role of individual T-cell populations on the development of mucous cells in mice following acrolein exposures is equivocal. Although there was a detectable number of mucous cells in the airways of mice that increased over time, the number of mucous cells was nominal compared with that observed following robust models of mucous cell metaplasia, such as those utilizing allergen sensitization and challenge (Borchers et al., 2001) or LPS inhalation (Vernooy et al., 2002). The failure of these assays to reveal insight into the role of αβ and γδ T cells in this phenotype is likely related to the relative resistance of mice to develop irritant-induced mucous cell metaplasia (Borchers et al., 1999).

In contrast to the requirement of γδ T cells in epithelial cell homeostasis, αβ T cells appear to be required for acrolein-induced macrophage accumulation. γδ-deficient mice exhibited a significant decrease in macrophage accumulation compared with C57BL/6J mice at 2 and 4 weeks of 2.0 ppm acrolein exposure, but were similar to C57BL/6J at 1 week of 2.0 ppm and all time points at 0.5 ppm acrolein. Strikingly, no increases in macrophage numbers were observed in αβ-deficient mice following either 2.0 or 0.5 ppm acrolein at any time points. The reasons for this effect are not clear, but may reflect the lack of critical cytokines/chemokines elaborated by T cells in response to a variety of inflammatory stimuli.

A major conclusion from these studies is that there is not a direct association between inflammation and epithelial cell pathologies in response to acrolein exposures. The maximum accumulation of BAL leukocytes was observed in the wild-type C57BL/6J mice, but maximal epithelial cell sloughing was observed in the γδ-deficient mice. This is somewhat surprising, as we would expect inflammation, especially related to macrophage accumulation, to increase with increased cellular damage in the airway lumen. The CASP3 staining reveals that the majority of cells undergoing apoptosis are in the distal airways and the airspaces. This is consistent with the BAL epithelial cell data that demonstrate that the majority of the epithelial cells are ciliated, meaning they are derived primarily from the proximal airways. Furthermore, the fact that it takes two weeks to develop significant numbers of apoptotic cells in the peripheral lung suggests that a low constant dose delivered to the distal airspaces can have deleterious effects not detectable at earlier time points. Regardless, these data suggest that epithelial cell pathology represents the major endpoint in terms of determining the function of γδ T cells in the response to acrolein exposure.

TABLE 2
Candidate Gene Expression Changes in $\gamma\delta^+$ T Cells following Acrolein Exposures

Accession ID	Gene symbol	Gene name	Description	Avg. intensity[a]	Fold induction[b]	p Value
BC061154	Chi3l3	Chitinase 3-like 3	Chitinase, promotes inflammation	630	13.39	0.0000001
L20315	Mpeg1	Macrophage expressed gene 1	Perforin-like activity	389	8.25	0.00001
BC005676	Cd44	CD44 antigen	Adhesion molecule	146	8.06	0.0002
NM_008013	Fgl2	Fibrinogen-like protein 2	T-cell regulation	183	5.91	0.00003
NM_007913	Egr1	Early growth response protein 1	T-cell differentiation	253	5.51	0.00001
NM_011210	Ptprc	Leukocyte common antigen precursor	Receptor signaling in T/B cells	12,668	5.19	0.0001
NM_013590	Lzps	Lysozyme C, type P	Antimicrobial enzyme	452	5.05	0.0003
NM_008871	Serpine1	Serine (or cysteine) peptidase inhibitor, clade E, member 1	Serine proteinase inhibitor	178	4.35	0.0002
NM_010511	Ifngr	Interferon gamma receptor alpha chain precursor	Interferon gamma receptor alpha chain	145	3.85	0.001
NM_016898	Cd164	CD164 antigen; cMyc binding protein	Adhesion molecule	1340	3.80	0.0003
NM_011613	Tnfsf11	Tumor necrosis factor ligand superfamily member 11	Mediate cytokine receptor cross-talk	996	3.68	0.0002
AF079527	Ier5	Immediate early response 5	Mediator of growth factor signaling	887	3.62	0.002
NM_009140	Cxcl2	Macrophage inflammatory protein 2	Neutrophil chemotaxis	4743	3.42	0.001
BC008565	Hmgb1	High mobility group box 1	TLR/RAGE agonist	332	3.39	0.0007
NM_007827	Daf2	Complement decay accelerating factor	Complement decay accelerating factor,	412	3.36	0.001
NM_007642	Cd28	T-cell–specific surface glycoprotein CD28	T-cell receptor coreceptor	17,742	3.13	0.002
NM_0010087	Il4ra	Interleukin 4 receptor alpha chain	IL-4 receptor alpha	323	3.11	0.004
NM_009841	Cd14	Monocyte differentiation antigen CD14	Toll receptor signaling	400	3.00	0.003
NM_008176	Cxcl1	Platelet-derived growth factor inducible protein KC	Chemokine	102	2.98	0.001
NM_008404	Itgb2	Integrin beta2	Adhesion molecule	180	2.79	0.004
NM_017480	Icos	Inducible T-cell costimulator	Inducible T-cell costimulator	1189	2.77	0.003
NM_177772	Bpl2	Bactericidal/permeability increasing protein-like 2	Antimicrobial protein	2978	2.61	0.003
NM_008462	Klra2	Killer cell lectin-like receptor 2	MHC-1 receptor	192	2.51	0.004
NM_053151	Klra9	Killer cell lectin-like receptor 9	MHC-1 receptor	732	−3.04	0.002
BC072560	Faim2	fas apoptotic inhibitory molecule 2	Apoptotic inhibitory molecule	97	−3.69	0.001
AK128979	Cxcl16	Chemokine (C-X-C motif) ligand 16	Chemokine	55	−3.28	0.003
NM_008002	Fgf10	Fibroblast growth factor 10	Growth factor	1207	−2.63	0.003
NM_032006	Mmp1a	Matrix metalloproteinase 1a	Matrix degradation	1486	−3.09	0.003

[a]Average intensity is an arbitrary value derived from the fluorescence intensity of the microarray analysis.
[b]Fold induction is the ratio of acrolein-exposed to sham-exposed values.

As with any genetically modified animals, the data and conclusions derived from mice genetically deficient in $\alpha\beta$ and $\gamma\delta$ T cells must be carefully interpreted. For example, we observed that mice deficient in $\alpha\beta$ T cells have a significant increase in the number of $\gamma\delta$ T cells in the lung. The consequences of this phenomenon are not well documented, but these alterations may subsequently affect the phenotype and, possibly, the function of these cells as well as other lymphocytes such as natural killer cells. This is especially important in the $\alpha\beta$-deficient mice in which a small change in the number of $\gamma\delta$ T cells may be amplified because they normally represent only 1–2% of the T-cell population. Furthermore, it is important to note that in the absence of $\gamma\delta$ T cells, $\alpha\beta$ T cells exhibit enhanced activity in terms of cytotoxicity and cytokine production (Lahn, 2000).

The goal of the microarray study was to characterize the differential response of tissue $\alpha\beta$ and $\gamma\delta$ T cells in the lungs following exposure to acrolein. We examined T-cell subpopulations isolated from the digested pulmonary tissue as opposed to peripheral blood because the effects of the local microenvironment can have profound effects on the phenotypes and effector functions of leukocytes. The transcriptional analyses revealed insight into the potential contributions of several genes in the regulation of inflammation and epithelial cell homeostasis.

The primary endpoint observed in the $\alpha\beta$ T-cell–deficient mice was a lack of increased macrophage accumulation. This phenotype was observed at both 0.5 and 2.0 ppm acrolein. Global gene expression analysis of purified $\alpha\beta$ T cells following acrolein exposure revealed that a number of genes involved in the accumulation and differentiation of macrophages were induced in this cell type. We hypothesize that the coordinated activities of IFN-γ, IL-12, IL-18, and additional chemokines/cytokines are critical components mediating the

TABLE 3
Validation of Microarray Changes by qRT-PCR

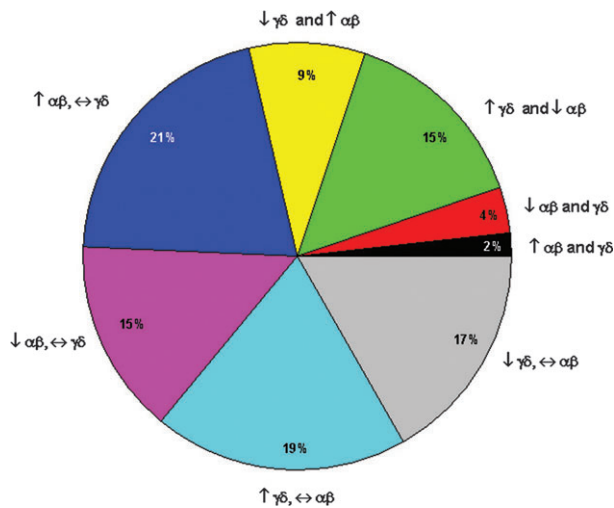| Gene symbol	αβ T cells (microarray)	αβ T cells (qRT-PCR)	γδ T cells (microarray)	γδ T cells (qRT-PCR)
Cd97	2.23	2.92	1.54	2.59
Hmgb1	1.28	1.33	3.39	1.96
CxCl2	1.43	11.76	3.42	4.25
Tnfsf11	0.64	0.68	3.68	2.33
Ifngr2	2.76	3.09	3.85	2.13
Egr1	0.64[a]	4.23[a]	5.51	2.65
Irf1	1.07	2.05	1.38	1.61
Ccl5	1.57	1.67	0.67	0.79
Ptprc	1.10	1.99	5.19	1.91
Cd164	0.61[a]	1.16[a]	3.80[a]	0.81[a]
S100a4	3.00	3.21	0.47	0.66
S100a10	1.35	0.99	0.78	0.64
Chi3l3	1.15	2.72	13.39[a]	0.86[a]
Klrc1	0.37	0.58	1.95	3.44
Il18r1	2.53	1.62	1.64[a]	0.53[a]

[a]Denotes values not confirmed by qRT-PCR.

cross-talk between T cells and tissue macrophages in response to acrolein-induced airway inflammation. IL-12 and IL-18 are cytokines produced predominantly by macrophages and act to stimulate T cells to, among other processes, generate cytokines such as granulocyte macrophage colony-stimulating factor and IFN-γ, which possess activating/survival properties on macrophages (Okamura *et al.*, 1998). IFN-γ possesses proliferative effects on T cells and induces IL-12 and IL-18 from macrophages in a processes shown to control inflammation and tissue destruction (Fantuzzi *et al.*, 2000; Trinchieri, 1998). This hypothesis is further supported by data demonstrating that

FIG. 6. Distinct patterns of gene expression in pulmonary αβ and γδ T cells following repeated acrolein exposures. Microarray analyses revealed that the majority of gene changes in each cell type were unique to that cell type. The percent of significant changes in mRNA levels are grouped and labeled as increased (↑), decreased (↓), or no change (↔).

patients with genetic deficiencies in *Ifngr2* display increased susceptibility to mycobacterial and *Listeria monocytogenes* infections, suggesting that this receptor is part of a critical pathway for elimination of pathogens and protection of the airways (Remus *et al.*, 2001). Additionally, T cells from *Ifngr2*−/− mice have a defect in Th1 cell differentiation and produce less amounts of IFN-γ in response to antigen challenge (Lu *et al.*, 1998). Moreover, Il18r1 has previously been demonstrated to play a role in development of inflammatory lung disease. Specifically, IL-18 and IL-18r1 signaling pathways are critical in the pathogenesis of cigarette smoke-induced pathologies, partly through the activation of pulmonary macrophages (Kang *et al.*, 2007).

Il3 represents another important gene upregulated in αβ T cells following acrolein exposures as it is a potent stimulator of macrophage differentiation and activation (Martinez-Moczygemba and Huston, 2003). Furthermore, Ccl5 (RANTES) and Scye1, potent mediators of macrophage accumulation and activation following tissue injury (Keepers *et al.*, 2007; Murdoch *et al.*, 2004), were among the highest expressed chemokines/cytokines detected in αβ T cells by our microarray analyses. Although the expression levels of these genes did not change, the lack of these cytokines in αβ-deficient mice may contribute to the significant decrease in macrophage accumulation observed in these mice. Significantly, an important role for the CCL5 receptor, CCR5, has been implicated in the long-term pulmonary pathologies due to cigarette smoke (Ma *et al.*, 2005).

The dominant phenotype observed in γδ T-cell–deficient mice following repeated acrolein exposures was increased sloughing of epithelial cells into the airways and increased expression of the apoptotic marker, active CASP3. Consistent with a previous report (King *et al.*, 1999), we observed an accumulation of necrotic epithelial cells in the airways of γδ-deficient mice following toxicant exposure. We have extended these findings by examining repeated exposures and assessing more subtle changes in the epithelium by measuring apoptosis. These data suggest that γδ-deficient mice fail to clear damaged or stressed cells, which attenuates the repair and repopulation of the airways with healthy cells. Global gene expression analysis of γδ T cells also revealed important insights into the function of these cells in maintaining the integrity of the epithelial barrier in the airways.

We hypothesize that this phenotype can be affected by multiple pathways including the attenuated recruitment of neutrophils and macrophage to clear necrotic cells, as well as the lack of clearance of stressed or apoptotic cells via MHC class 1- and MHC class 1–like mediated mechanisms. This is supported by the increase in genes associated with neutrophil accumulation (*Cxcl1* and *Cxcl2*), and the changes in genes associated with the recognition of MHC-1 receptors (*Klra2*, *Klra9*, *Mpeg1*) on target cells. Although less characterized for their roles in tissue remodeling, genes such as *Cd14* (Jiang *et al.*, 2006) and *Cd44* (Teder *et al.*, 2002), which are upregulated

in γδ T cells, have also been implicated in the response to pulmonary injury and the resolution of inflammation.

In addition to the potential roles of genes that are significantly changed in γδ T cells following acrolein exposures, transcriptome analyses indicated that these cells express significant levels of > 20 genes involved in the recognition and removal of injured tissue. These genes included 12 killer cell lectin-like receptors (MHC-1 receptors), *Ncr1* (a natural cytotoxicity receptor), and *Itcst* (cytotoxicity receptor signaling adaptor). These genes are of particular importance because previous studies in our lab have demonstrated that MHC-1 expression decreased on epithelial cells coincident with stress/injury and this is accompanied by the induction of stress signals on the surface of epithelial cells (Borchers *et al.*, 2006). These findings, along with their localization within the pulmonary epithelium (Wands *et al.*, 2005), are consistent with the idea that γδ T cells are critical for efficient removal of stressed or injured cells following acrolein exposure through the loss of self recognition and the expression of danger signals (Hayday *et al.*, 2001). Furthermore, It has been suggested that fibroblast growth factor (*Fgf7*), due to potent effects on epithelial cell survival, may account for the protective effect of γδ T cells in response to injury or infection (Baba *et al.*, 2007; Hokuto *et al.*, 2004). However, we observed no differences in Fgf7 mRNA levels in the whole lungs of C57BL/6J, αβ-deficient, or γδ-deficient mice at baseline or following repeated acrolein exposures (data not shown).

Taken together, these results provide compelling evidence to support the hypotheses that (1) αβ T cells are critical for the initial and sustained accumulation of macrophages following repeated acrolein exposures, and (2) γδ T cells serve a protective role in the lung to maintain the integrity of the airway epithelium in response to repeated acrolein exposures. Although we present direct and indirect evidence of a role for αβ and γδ T cells in these phenotypes, the mechanisms remain to be determined. However, these findings provide a strong rationale to dissect the effector functions of these cells in the modulation of lung pathophysiology.

REFERENCES

Augustin, A., and Sim, G. K. (1990). Positive selection and extrathymic expansion of gamma delta T cells. *Res. Immunol.* **141,** 593–595.

Baba, Y., Yazawa, T., Kanegae, Y., Sakamoto, S., Saito, I., Morimura, N., Goto, T., Yamada, Y., and Kurahashi, K. (2007). Keratinocyte growth factor gene transduction ameliorates acute lung injury and mortality in mice. *Hum. Gene Ther.* **18,** 130–141.

Bleavins, M. R., Sargent, N. E., and Dziedzic, D. (1995). Effects of cyclosporine A on ozone-induced pulmonary lesion formation: Pharmacologic elimination of the T-lymphocyte regulatory response. *Arch. Environ. Contam. Toxicol.* **28,** 240–247.

Boismenu, R., and Havran, W. L. (1994). Modulation of epithelial cell growth by intraepithelial gamma delta T cells. *Science* **266,** 1253–1255.

Borchers, M. T., Crosby, J., Farmer, S., Sypek, J., Ansay, T., Lee, N. A., and Lee, J. J. (2001). Blockade of CD49d inhibits allergic airway pathologies independent of effects on leukocyte recruitment. *Am. J. Physiol. Lung Cell. Mol. Physiol.* **280,** L813–L821.

Borchers, M. T., Harris, N. L., Wesselkamper, S. C., Vitucci, M., and Cosman, D. (2006). NKG2D ligands are expressed on stressed human airway epithelial cells. *Am. J. Physiol. Lung Cell. Mol. Physiol.* **291,** L222–L231.

Borchers, M. T., Wert, S. E., and Leikauf, G. D. (1998). Acrolein-induced MUC5ac expression in rat airways. *Am. J. Physiol.* **274,** L573–L581.

Borchers, M. T., Wesselkamper, S., Wert, S. E., Shapiro, S. D., and Leikauf, G. D. (1999). Monocyte inflammation augments acrolein-induced Muc5ac expression in mouse lung. *Am. J. Physiol.* **277,** L489–L497.

Borchers, M. T., Wesselkamper, S. C., Harris, N. L., Deshmukh, H., Beckman, E., Vitucci, M., Tichelaar, J. W., and Leikauf, G. D. (2007a). CD8(+) T cells contribute to macrophage accumulation and airspace enlargement following repeated irritant exposure. *Exp. Mol. Pathol.* **83,** 301–310.

Borchers, M. T., Wesselkamper, S. C., Harris, N. L., Deshmukh, H., Beckman, E., Vitucci, M., Tichelaar, J. W., and Leikauf, G. D. (2007b). CD8+ T cells contribute to macrophage accumulation and airspace enlargement following repeated irritant exposure. *Exp. Mol. Pathol.* **83,** 301–310.

Caldwell, J. C., Woodruff, T. J., Morello-Frosch, R., and Axelrad, D. A. (1998). Application of health information to hazardous air pollutants modeled in EPA's Cumulative Exposure Project. *Toxicol. Ind. Health* **14,** 429–454.

Carmines, E. L., and Rajendran, N. (2008). Evidence for carbon monoxide as the major factor contributing to lower fetal weights in rats exposed to cigarette smoke. *Toxicol. Sci.* **102,** 383–391.

Chen, X., Gavett, S. H., and Wills-Karp, M. (1995). CD4+ T lymphocyte modulation of ozone-induced murine pulmonary inflammation. *Am. J. Respir. Cell. Mol. Biol.* **12,** 396–403.

Cohen, I. R.a A. P. A. (1961). A new spectrophotometric method for the determination of acrolein in combustion gases and in the atmosphere. *Anal. Chem.* **33,** 726–733.

Costa, D. L., Kutzman, R. S., Lehmann, J. R., and Drew, R. T. (1986). Altered lung function and structure in the rat after subchronic exposure to acrolein. *Am. Rev. Respir. Dis.* **133,** 286–291.

Dziedzic, D., and White, H. J. (1987). Response of T-cell-deficient mice to ozone exposure. *J. Toxicol. Environ. Health* **21,** 57–71.

Fahrer, A. M., Konigshofer, Y., Kerr, E. M., Ghandour, G., Mack, D. H., Davis, M. M., and Chien, Y. H. (2001). Attributes of gammadelta intraepithelial lymphocytes as suggested by their transcriptional profile. *Proc. Natl. Acad. Sci. U. S. A.* **98,** 10261–10266.

Fantuzzi, L., Puddu, P., Varano, B., Del Corno, M., Belardelli, F., and Gessani, S. (2000). IFN-alpha and IL-18 exert opposite regulatory effects on the IL-12 receptor expression and IL-12-induced IFN-gamma production in

mouse macrophages: Novel pathways in the regulation of the inflammatory response of macrophages. *J. Leukoc. Biol.* **68,** 707–714.

Feron, V. J., Kruysse, A., Til, H. P., and Immel, H. R. (1978). Repeated exposure to acrolein vapour: Subacute studies in hamsters, rats and rabbits. *Toxicology* **9,** 47–57.

Hayday, A., Theodoridis, E., Ramsburg, E., and Shires, J. (2001). Intra-epithelial lymphocytes: Exploring the Third Way in immunology. *Nat. Immunol.* **2,** 997–1003.

Hokuto, I., Perl, A. K., and Whitsett, J. A. (2004). FGF signaling is required for pulmonary homeostasis following hyperoxia. *Am. J. Physiol. Lung Cell. Mol. Physiol.* **286,** L580–L587.

Jiang, D., Liang, J., Li, Y., and Noble, P. W. (2006). The role of Toll-like receptors in non-infectious lung injury. *Cell Res.* **16,** 693–701.

Kang, M. J., Homer, R. J., Gallo, A., Lee, C. G., Crothers, K. A., Cho, S. J., Rochester, C., Cain, H., Chupp, G., Yoon, H. J., *et al.* (2007). IL-18 is induced and IL-18 receptor alpha plays a critical role in the pathogenesis of cigarette smoke-induced pulmonary emphysema and inflammation. *J. Immunol.* **178,** 1948–1959.

Keepers, T. R., Gross, L. K., and Obrig, T. G. (2007). Monocyte chemoattractant protein 1, macrophage inflammatory protein 1 alpha, and RANTES recruit macrophages to the kidney in a mouse model of hemolytic-uremic syndrome. *Infect. Immun.* **75,** 1229–1236.

Kehrer, J. P., and Biswal, S. S. (2000). The molecular effects of acrolein. *Toxicol. Sci.* **57,** 6–15.

King, D. P., Hyde, D. M., Jackson, K. A., Novosad, D. M., Ellis, T. N., Putney, L., Stovall, M. Y., Van Winkle, L. S., Beaman, B. L., and Ferrick, D. A. (1999). Cutting edge: Protective response to pulmonary injury requires gamma delta T lymphocytes. *J. Immunol.* **162,** 5033–5036.

Lahn, M. (2000). The role of gammadelta T cells in the airways. *J. Mol. Med.* **78,** 409–425.

Leikauf, G. D. (2002). Hazardous air pollutants and asthma. *Environ. Health Perspect.* **110**(Suppl. 4), 505–526.

Lu, B., Ebensperger, C., Dembic, Z., Wang, Y., Kvatyuk, M., Lu, T., Coffman, R. L., Pestka, S., and Rothman, P. B. (1998). Targeted disruption of the interferon-gamma receptor 2 gene results in severe immune defects in mice. *Proc. Natl. Acad. Sci. U. S. A.* **95,** 8233–8238.

Lyon, J. P., Jenkins, L. J., Jr., Jones, R. A., Coon, R. A., and Siegel, J. (1970). Repeated and continuous exposure of laboratory animals to acrolein. *Toxicol. Appl. Pharmacol.* **17,** 726–732.

Ma, B., Kang, M. J., Lee, C. G., Chapoval, S., Liu, W., Chen, Q., Coyle, A. J., Lora, J. M., Picarella, D., Homer, R. J., *et al.* (2005). Role of CCR5 in IFN-gamma-induced and cigarette smoke-induced emphysema. *J. Clin. Invest.* **115,** 3460–3472.

Martinez-Moczygemba, M., and Huston, D. P. (2003). Biology of common beta receptor-signaling cytokines: IL-3, IL-5, and GM-CSF. *J. Allergy Clin. Immunol.* **112,** 653– 665; quiz 666.

Miller, L. M., Foster, W. M., Dambach, D. M., Doebler, D., McKinnon, M., Killar, L., and Longphre, M. (2002). A murine model of cigarette smoke-induced pulmonary inflammation using intranasally administered smoke-conditioned medium. *Exp. Lung Res.* **28,** 435–455.

Murdoch, C., Giannoudis, A., and Lewis, C. E. (2004). Mechanisms regulating the recruitment of macrophages into hypoxic areas of tumors and other ischemic tissues. *Blood* **104,** 2224–2234.

Okamura, H., Kashiwamura, S., Tsutsui, H., Yoshimoto, T., and Nakanishi, K. (1998). Regulation of interferon-gamma production by IL-12 and IL-18. *Curr. Opin. Immunol.* **10,** 259–264.

Remus, N., Reichenbach, J., Picard, C., Rietschel, C., Wood, P., Lammas, D., Kumararatne, D. S., and Casanova, J. L. (2001). Impaired interferon gamma-mediated immunity and susceptibility to mycobacterial infection in child-hood. *Pediatr. Res.* **50,** 8–13.

Shires, J., Theodoridis, E., and Hayday, A. C. (2001). Biological insights into TCRgammadelta+ and TCRalphabeta+ intraepithelial lymphocytes pro-vided by serial analysis of gene expression (SAGE). *Immunity* **15,** 419–434.

Smyth, G. K. (2004). Linear models and empirical Bayes methods for assessing differential expression in microarray experiments. *Stat. Appl. Genet. Mol. Biol.* **3,** Article 3.

Stevens, J. F., and Maier, C. S. (2008). Acrolein: Sources, metabolism, and biomolecular interactions relevant to human health and disease. *Mol. Nutr. Food Res.* **52,** 7–25.

Teder, P., Vandivier, R. W., Jiang, D., Liang, J., Cohn, L., Pure, E., Henson, P. M., and Noble, P. W. (2002). Resolution of lung inflammation by CD44. *Science* **296,** 155–158.

Trinchieri, G. (1998). Immunobiology of interleukin-12. *Immunol. Res.* **17,** 269–278.

U.S. EPA. (2006). The 1999 National-Scale Air Toxics Assessment. Available at: http://www.epa.gov/ttn/atw/natamain/ [accessed 5 February 2008].

Vernooy, J. H., Dentener, M. A., van Suylen, R. J., Buurman, W. A., and Wouters, E. F. (2002). Long-term intratracheal lipopolysaccharide exposure in mice results in chronic lung inflammation and persistent pathology. *Am. J. Respir. Cell. Mol. Biol.* **26,** 152–159.

Wands, J. M., Roark, C. L., Aydintug, M. K., Jin, N., Hahn, Y. S., Cook, L., Yin, X., Dal Porto, J., Lahn, M., Hyde, D. M., *et al.* (2005). Distribution and leukocyte contacts of gammadelta T cells in the lung. *J. Leukoc. Biol.* **78,** 1086–1096.

Wesselkamper, S. C., Case, L. M., Henning, L. N., Borchers, M. T., Tichelaar, J. W., Mason, J. M., Dragin, N., Medvedovic, M., Sartor, M. A., Tomlinson, C. R., *et al.* (2005). Gene expression changes during the development of acute lung injury role of transforming growth factor {beta}. *Am. J. Respir. Crit. Care Med.* **172,** 1399–1411.

Wolfinger, R. D., Gibson, G., Wolfinger, E. D., Bennett, L., Hamadeh, H., Bushel, P., Afshari, C., and Paules, R. S. (2001). Assessing gene significance from cDNA microarray expression data via mixed models. *J. Comput. Biol.* **8,** 625–637.

Woodruff, T. J., Wells, E. M., Holt, E. W., Burgin, D. E., and Axelrad, D. A. (2007). Estimating risk from ambient concentrations of acrolein across the United States. *Environ. Health Perspect.* **115,** 410–415.